Effectiveness of Reducing Home VOC Measurements using One Inch Carbon Furnace Filters

Adayshia Haddock-Pitt, Dr. Barbara J. Polikva, Russ Barnett
University of Louisville School of Nursing

Introduction

- Exposure to high levels of carcinogens may lead to kidney, liver, or central nervous system damage
- Volatile Organic Compounds (VOC's) such as Acrolein, Carbon Tetrachloride, Benzene, and Chloroform are carcinogenic at high levels.
  - ❖Benzene is in paints and industrial solvents
  - ❖Acrolein is in gasoline and cooking oils.
  - ❖Chloroform is in tap water, swimming pools, and drinking water.
  - ❖Carbon Tetrachloride is in aerosol propellants, dry cleaning, varnish, lacquer, plastic glue, plastic bonders

Hypothesis

The activated carbon furnace filters will reduce the postliminary VOC levels.

Objective

This study used one inch carbon furnace filters to determine if the there is a difference between baseline and postliminary carcinogenic VOC readings in homes of older adults with asthma.

Preliminary Data

In an ongoing study examining the homes of older adults with asthma for asthma triggers, eighty-five VOC's including Carbon Tetrachloride, Benzene, Chloroform, and Acrolein were measured over 24 hours.

Methods

- A case study approach was used with 2 participants in the asthma study volunteered their home for VOC data collection using 1" carbon furnace filters.
- A One Inch Filtrete Allergen Plus Odor Reduction Air and Furnace Filter that contains activated carbon was carefully placed in the furnace of each home.
  - ❖ Activated carbon removes impurities in the air from unwanted chemicals, including VOCs
- Grab samples were obtained at 8-day and 15-day period using the Summa Canisters (See picture).
- VOC samples were analyzed by gas chromatography/mass spectrometry in full scan mode according to US EPA method TO-15, using a quadrapole GC (HP 6890) with a HP 5973 Mass Selective Detector.
- Data were graphically depicted to determine changes in ppb of total VOCs, Acrolein, Carbon Tetrachloride, Benzene, and Chloroform from baseline to postliminary data.

Results

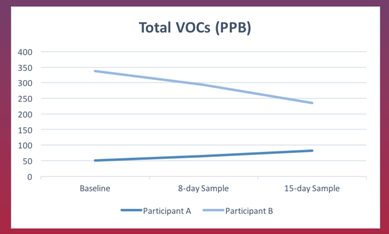

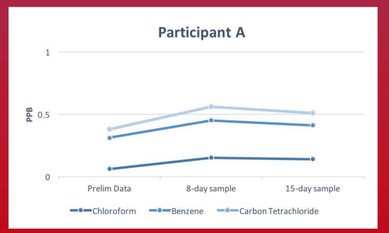

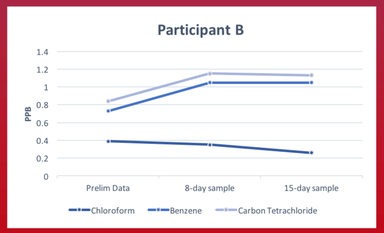

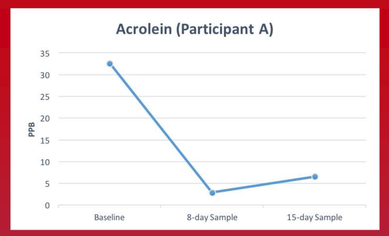

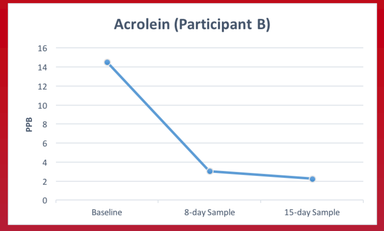

Conclusions

- The hypothesis was supported only by findings from the home of Participant A for Total VOC ppb, Chloroform ppb from the home of Participant B, and Acrolein from the home of both participants.
- Findings from these two case studies do not support the use of 1" carbon filters to consistently reduce carcinogenic VOCs.
- Future studies should investigate the use of 4" carbon filters and carbon air filtration systems in reducing VOCs in homes.
- Future studies should increase the number of participants and extend the evaluation time to at least 1 month.

Acknowledgements

Research supported by a grant from R25-CA134283 grant from the National Cancer Institute. And by the National Institute on Aging under Award Number R01AG047297. The content is solely the responsibility of the authors and does not necessarily represent the official views of the National Institutes of Health.

Healthy Lifestyle Impact on Breast Cancer-Specific and All-Cause Mortality

Adaline E. Heitz[1], Stephanie D. Boone, PhD, MPH[2], Delvon T. Mattingly, B.S.[1], Richard N. Baumgartner, PhD[2], Kathy B. Baumgartner, PhD[2]

R25 Program[1] and Department of Epidemiology & Population Health, School of Public Health & Information Sciences, and James Graham Brown Cancer Center[2]

Introduction

Despite recent advancements in early detection and treatment, breast cancer still remains the second leading cause of death for women in the U.S. [1]. Individual lifestyle factors have long been associated with cancer mortality, with national organizations like the American Cancer Society (ACS) going so far as to issue cancer prevention recommendations for many modifiable factors, including smoking, physical activity, body size and shape, alcohol consumption, and diet [2]. Several studies have evaluated the combined impact of these factors on cancer mortality through the creation of a Healthy Behavior Index (HBI); however, associations between the index and mortality among cancer survivors have been inconsistent [3-6]. Few studies have attempted to use the HBI to evaluate the impact of these factors on mortality in minority cancer populations. Hispanic (H) women have a higher risk of breast cancer-specific mortality than Non-Hispanic White (NHW) women, making this U.S. population one of particular interest [7].

The primary objective of this study was to evaluate the combined effect of healthy lifestyle factors on breast cancer-specific and all-cause mortality in NHW and H women included in the New Mexico site of the 4-Corners Women's Health Study through the construction of a HBI. Based on the findings of past studies, we hypothesized the HBI would be associated with breast cancer-specific and all-cause mortality in both ethnic groups [3-6].

Methods

New Mexico Site of 4-Corners Women's Health Study (1999-2005)

Study Objective
- To gain a better understanding of the etiology of breast cancer among Hispanic and NHW women

Case Inclusion Criteria
- Self-reported Hispanic, American Indian, or NHW ethnicity
- New Mexico resident
- 25-79 years of age
- Histologically confirmed first primary *in-situ* or invasive breast cancer diagnosis between October 1999 and May 2004
- Initial ascertainment from state tumor registries (SEER) with subsequent screenings to confirm eligibility

Data Collection
- Comprehensive diet and lifestyle data for the year prior to diagnosis collected by interviewer-administered computerized questionnaires
- Weight, height, and waist/hip circumference measured at time of interview
- Blood/saliva collected at time of interview

Variable	Definition	Description
All-cause mortality	Deceased any cause	Dependent/ Outcome
Breast-cancer specific mortality	ICD C50 COD	Dependent/ Outcome
Smoking status	0= Never 1= Former 2= Current	Independent/ HBI Component
Body mass index (kg/m²)	0= Normal, <25 1= Overweight, 25-30 2= Obese, ≥30	Independent/ HBI Component
Waist to hip ratio (inches)	0= <0.775 1= 0.775-0.84 2= ≥0.84	Independent/ HBI Component
Alcohol consumption (std drinks/ day)	0= ≤0.5 1= 0.5-1 2= >1	Independent/ HBI Component
Dietary Pattern*	0= T1 2= T2 3= T3	Independent/ HBI Component
Vigorous physical activity (min/week)	0= >75 1= ≤75 2= none	Independent/ HBI Component
Healthy behavior index	Q1= 0-3 Q2= 4-5 Q3= 6-7 Q4= 8-12	Independent/ Main Effect

* High in dairy fat, refined grains, snacks, gravies and sauces, potatoes, bacon, beef, sugary drinks and desserts, prepared foods, and fast foods; low in fresh fruits and vegetables [8]

Statistical Analysis (using SAS Version 9.4; Cary, NC)
- The dataset was restricted to cases with regional or distant cancer for the analytic sample (*n*=837), excluding outliers (*n*=4) and *in-situ* cases (*n*=151).
- HBI components were categorized based on distribution in controls (diet, waist to hip ratio), ACS cancer prevention guidelines (alcohol consumption, physical activity), and standard cut-points (BMI, smoking status).
- An HBI score (0-12) was calculated by adding scores (0-2) for individual components.
- Descriptive statistics for demographic and prognostic variables were calculated and compared by HBI quartiles; differences were assessed using chi-square test.
- Cox proportional hazards multivariable modeling was used to estimate hazard ratios (HR) and 95% confidence intervals (CI) for HBI quartiles, adjusting for stage at diagnosis and education.
- Effect modification was evaluated by self-reported ethnicity and stage at diagnosis.
- A Kaplan-Meier curve was constructed in order to illustrate survival over time by HBI quartiles and a log-rank p-value was used to determine differences in survival time.

Results

Table 1: Descriptive statistics for demographic and prognostic variables by healthy behavior index quartiles

	Healthy Behavior Index								
	Q1 (0-3)		Q2 (4-5)		Q3 (6-7)		Q4 (8-12)		
Characteristic	*n*=208		*n*=284		*n*=243		*n*=102		*p*[a]
Age (yrs; mean±SD)	53.1±11.3		56.2±11.7		55.5±12.1		56.1±11.2		0.02
Survival (yrs; mean±SD)	10.3±2.5		10.3±2.7		10.1±2.6		9.5±3.4		0.046
	n	%	*n*	%	*n*	%	*n*	%	
Race									0.02
Non-Hispanic White	145	69.7	187	65.9	138	56.8	70	68.6	
Hispanic	63	30.3	97	34.2	105	43.2	32	31.4	
Education									
<High school	13	6.3	29	10.2	38	15.6	17	16.7	0.0002
High school/GED	36	17.3	70	24.7	70	28.8	28	27.5	
>High school	159	76.4	183	64.4	135	55.6	57	55.9	
Menopausal status									0.005
Premenopausal	96	46.2	93	32.8	83	34.2	30	29.4	
Postmenopausal	112	53.9	191	67.3	160	65.8	72	70.6	
Smoking Status									<.0001
Never	153	73.6	164	57.8	125	51.4	17	16.7	
Former	48	23.1	86	30.3	70	28.8	42	41.2	
Current	7	3.4	34	12.0	48	19.8	43	42.2	
Body Mass Index (kg/m²)									<.0001
Normal, <25	165	79.3	136	47.9	50	20.6	11	10.8	
Overweight, 25-30	41	19.7	113	39.8	96	39.5	35	34.3	
Obese, ≥30	2	0.96	35	12.3	97	39.9	56	54.9	
Alcohol Consumption (std drinks/day)									<.0001
≤0.5	186	89.4	237	83.5	199	81.9	65	63.7	
0.5-1	19	9.1	26	9.2	19	7.8	13	12.8	
>1	3	1.4	21	7.4	25	10.3	24	23.5	
Vigorous Physical Activity (min/wk)									<.0001
>75	110	52.9	68	23.9	32	13.2	2	2.0	
≤75	64	30.8	107	37.7	79	32.5	15	14.7	
None	34	16.4	109	38.4	132	54.3	85	83.3	
Dietary Pattern									<.0001
T1	107	51.4	88	31.0	30	12.4	2	2.0	
T2	82	39.4	118	41.6	90	37.0	26	25.5	
T3	19	9.1	78	27.5	123	50.6	74	72.6	
Waist to Hip Ratio (inches)									<.0001
<0.775	130	62.5	70	24.7	24	9.9	3	2.9	
0.775-0.84	67	32.2	140	49.3	78	32.1	18	17.7	
≥0.84	11	5.3	74	26.1	141	58.0	81	79.4	
Stage									0.53
Localized	140	67.3	196	69.0	159	65.4	65	63.7	
Regional	64	30.8	84	29.6	77	31.7	37	36.3	
Distant	3	1.4	3	1.1	6	2.5	0	0	
ER Status									0.97
ER+	116	56.0	163	57.6	129	53.3	58	56.7	
ER-	35	16.9	45	15.9	42	17.3	18	17.7	

Note: Column percentages (%) may not add up to 100% due to rounding or missing observations. Column totals (n) may not add up to total due to missing observations: education (n=2), stage (n=3), and ER status (n=228).
[a] Comparisons between HBI quartiles; p-values reported for Mantel-Haenszel chi-square (categorical) and ANOVA (continuous).

Table 2: Associations between healthy behavior index and breast cancer-specific and all-cause mortality, stratified by race

Breast Cancer-Specific Mortality	All Women			Non-Hispanic White			Hispanic		
	Deaths/No	Crude HR (95% CI)	Adjusted HR[a] (95% CI)	Deaths/No	Crude HR (95% CI)	Adjusted HR[a] (95% CI)	Deaths/No	Crude HR (95% CI)	Adjusted HR[a] (95% CI)
Healthy Behavior Index									
Q1 (0-3)	23/207	1.00	1.00	15/144	1.00	1.00	8/63	1.00	1.00
Q2 (4-5)	31/283	1.00 (0.58-1.71)	0.98 (0.57-1.68)	17/186	0.89 (0.44-1.78)	0.91 (0.45-1.82)	14/97	1.17 (0.49-2.79)	1.13 (0.47-2.70)
Q3 (6-7)	31/242	1.19 (0.69-2.04)	1.04 (0.60-1.81)	16/137	1.91 (0.59-2.41)	1.19 (0.58-2.45)	15/105	1.12 (0.47-2.64)	0.97 (0.41-2.31)
Q4 (8-12)	13/102	1.27 (0.65-2.52)	1.15 (0.58-2.28)	8/70	1.30 (0.55-3.06)	1.25 (0.52-2.98)	5/32	1.28 (0.42-3.91)	1.27 (0.41-3.88)
p-trend		*0.79*	*0.68*		*0.43*	*0.50*		*0.73*	*0.89*
p-interaction[b]									*0.94*
All-Cause Mortality	**All Women**			**Non-Hispanic White**			**Hispanic**		
	Deaths/No	Crude HR (95% CI)	Adjusted HR[a] (95% CI)	Deaths/No	Crude HR (95% CI)	Adjusted HR[a] (95% CI)	Deaths/No	Crude HR (95% CI)	Adjusted HR[a] (95% CI)
Healthy Behavior Index									
Q1 (0-3)	36/207	1.00	1.00	26/144	1.00	1.00	10/63	1.00	1.00
Q2 (4-5)	63/283	1.28 (0.85-1.93)	1.19 (0.79-1.80)	40/186	1.21 (0.74-1.98)	1.19 (0.72-1.95)	23/97	1.51 (0.72-3.17)	1.29 (0.61-2.74)
Q3 (6-7)	51/242	1.27 (0.83-1.95)	1.11 (0.72-1.72)	27/137	1.20 (0.70-2.07)	1.14 (0.66-1.98)	24/105	1.42 (0.68-2.98)	1.18 (0.56-2.50)
Q4 (8-12)	39/102	2.44 (1.55-3.85)	2.18 (1.37-3.44)	30/70	2.90 (1.71-4.91)	2.65 (1.54-4.55)	9/32	1.75 (0.71-4.31)	1.63 (0.66-4.03)
p-trend		*0.0008*	*0.006*		*0.0005*	*0.002*		*0.2887*	*0.43*
p-interaction[b]									*0.60*

[a] Adjusted for education and stage at diagnosis [b] Interaction reported for HBI quartile and race

Table 3: Associations between healthy behavior index and breast cancer-specific and all-cause mortality, stratified by stage at diagnosis

Breast Cancer-Specific Mortality	Localized			Regional/Distant		
	Deaths/No	Crude HR (95% CI)	Adjusted HR[a] (95% CI)	Deaths/No	Crude HR (95% CI)	Adjusted HR[a] (95% CI)
Healthy Behavior Index						
Q1 (0-3)	10/140	1.00	1.00	13/67	1.00	1.00
Q2 (4-5)	11/196	0.79 (0.34-1.86)	0.72 (0.30-1.70)	20/87	1.21 (0.60-2.43)	1.18 (0.57-2.39)
Q3 (6-7)	11/159	0.98 (0.42-2.31)	0.83 (0.35-2.00)	20/83	1.33 (0.66-2.67)	1.21 (0.59-2.48)
Q4 (8-12)	3/65	0.68 (0.19-2.47)	0.56 (0.15-2.05)	10/37	1.66 (0.73-3.79)	1.59 (0.70-3.65)
p-trend		*0.7349*	*0.48*		*0.2252*	*0.32*
p-interaction[b]						*0.65*
All-Cause Mortality	**Localized**			**Regional/Distant**		
	Deaths/No	Crude HR (95% CI)	Adjusted HR[a] (95% CI)	Deaths/No	Crude HR (95% CI)	Adjusted HR[a] (95% CI)
Healthy Behavior Index						
Q1 (0-3)	22/140	1.00	1.00	14/67	1.00	1.00
Q2 (4-5)	37/196	1.21 (0.72-2.06)	1.09 (0.64-1.87)	26/87	1.43 (0.75-2.75)	1.38 (0.72-2.66)
Q3 (6-7)	26/159	1.10 (0.62-1.94)	0.97 (0.54-1.72)	25/83	1.53 (0.79-2.94)	1.36 (0.70-2.67)
Q4 (8-12)	22/65	2.29 (1.27-4.14)	1.94 (1.06-3.57)	17/37	2.62 (1.29-5.31)	2.49 (1.22-5.08)
p-trend		*0.0287*	*0.099*		*0.0130*	*0.03*
p-interaction[b]						*0.92*

[a] Adjusted for education [b] Interaction reported for HBI quartile and stage

Figure 1: Breast Cancer Survival by HBI Quartiles

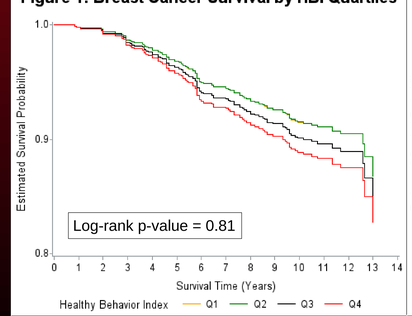

Breast Cancer Survival Rate	Q1	Q2	Q3	Q4
	84%	85%	86%	77%

Figure 2: Overall Survival by HBI Quartiles

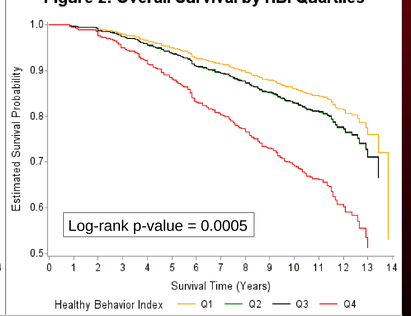

Overall Survival Rate	Q1	Q2	Q3	Q4
	70%	71%	71%	53%

References

1. Howlader, N., et al., SEER Cancer Statistics Review, 1975-2013: National Cancer Institute. Bethesda, MD. http://seer.cancer.gov/csr/1975_2013/, November 2015 SEER data submission, posted to the SEER web site, April 2016
2. Kushi, L., et al. (2006). American Cancer Society Guidelines on Nutrition and Physical Activity for Cancer Prevention: Reducing the Risk of Cancer With Healthy Food Choices and Physical Activity. CA: A Cancer Journal for Clinicians, 56(5), 254-281.
3. Khaw, K., et al. (2008). Combined Impact of Health Behaviours and Mortality in Men and Women: The EPIC-Norfolk Prospective Population Study. PLoS Med PLoS Medicine, 5(1).
4. Kohler, L., et al. (2016). Adherence to Diet and Physical Activity Cancer Prevention Guidelines and Cancer Outcomes: A Systematic Review. Cancer Epidemiology Biomarkers & Prevention, 25(7), 1018-1028.
5. Mccullough, M., et al. (2011). Following Cancer Prevention Guidelines Reduces Risk of Cancer, Cardiovascular Disease, and All-Cause Mortality. Cancer Epidemiology Biomarkers & Prevention, 20(6), 1089-1097.
6. Petersen, K., et al. (2015). The combined impact of adherence to five lifestyle factors on all-cause, cancer and cardiovascular mortality: A prospective cohort study among Danish men and women. British Journal of Nutrition Br J Nutr, 113(05), 849-858.
7. Boone, S., et al. (2013). The joint contribution of tumor phenotype and education to breast cancer survival disparity between Hispanic and non-Hispanic white women. Cancer Causes & Control Cancer Causes Control, 25(3), 273-282.
8. Murtaugh, M., et al. (2007). Diet Composition and Risk of Overweight and Obesity in Women Living in the Southwestern United States Journal of the American Dietetic Association, 107(8), 1311-1321.

Acknowledgements

Research support:
NCI R25-CA134283;
NIH/NCI R01-CA78762;
James Graham Brown Cancer Center

Conclusions

- Survival rates were lowest for HBI Q4 for breast cancer survival and overall survival (77% and 53%, respectively) and significantly differed from other HBI quartiles for overall survival (log-rank p=0.0005).
- An increased risk of breast cancer-specific mortality for HBI Q2-Q4 compared to Q1 was present, but was not statistically significant overall, by ethnicity or stage of disease.
- A significant >2-fold increased risk of all-cause (AC) mortality was observed for all women and NHW women in HBI Q4 *vs.* Q1.
- AC mortality did not differ by stage of disease; however, the association of HBI with AC mortality was stronger in women with regional/distant stage.
- A significant increasing trend across HBI quartiles was observed among all women, NHW women, and those diagnosed with localized or regional/distant stage of disease for AC mortality.
- An increasing number of unhealthy lifestyle factors influences AC mortality among breast cancer survivors, which can primarily be attributed to cardiovascular and pulmonary diseases.
- Interventions for breast cancer survivors should address the combination of lifestyle factors and their effect on prognosis, recurrence, and second primaries.

Investigating HGPRT as a Component of an AS1411 Prodrug Mechanism

Parker T. Howard, Sarah A. Andres, Paula J. Bates
Department of Medicine, University of Louisville, Louisville, KY 40202

Abstract

AS1411 is a guanine-rich oligonucleotide with antiproliferative activity in numerous cancer cell lines. It has previously been tested in human clinical trials and has induced dramatic clinical responses in a few patients.1,2 AS1411 acts as an aptamer that binds to nucleolin, a protein expressed selectively on the surface of cancer cells, but its precise mechanism of action is not yet fully understood.1 Recent literature has suggested that degradation of AS1411 to its constituent nucleotides may play a role.3 In particular, guanine based purine compounds (GBPCs) are capable of significantly inhibiting cancerous growth in vitro,3,4 suggesting that AS1411 may function as a "prodrug" for guanine. It has been shown previously that the antiproliferative effects of GBPCs are dependent on the activity of hypoxanthine-guanine phosphoribosyltransferase (HGPRT), an enzyme involved in the purine salvage pathway.4 **We reasoned that if AS1411 is acting as a prodrug for guanine then its activity should also depend on HGPRT.** To test this possibility, A549 lung cancer cells were left untransfected, transfected with HGPRT siRNA, or transfected with a negative control siRNA prior to treatment with either AS1411, CRO (a cytosine-rich negative control oligonucleotide), or sterile water (vehicle control). Cells were then evaluated using the MTT colorimetric assay to determine relative levels of cellular proliferation. We found that AS1411 retained its antiproliferative properties even when HGPRT levels were depleted by siRNA knockdown. Several parameters were varied, such as transfection time, treatment time, and siRNA concentration, but the results remained consistent. These data indicate that AS1411 antiproliferative effects are not dependent on HGPRT and suggest that AS1411 activity is not be related to GBPCs in this cell line. However, further studies to explore the relationship between AS1411 and GBPCs are warranted.

Background

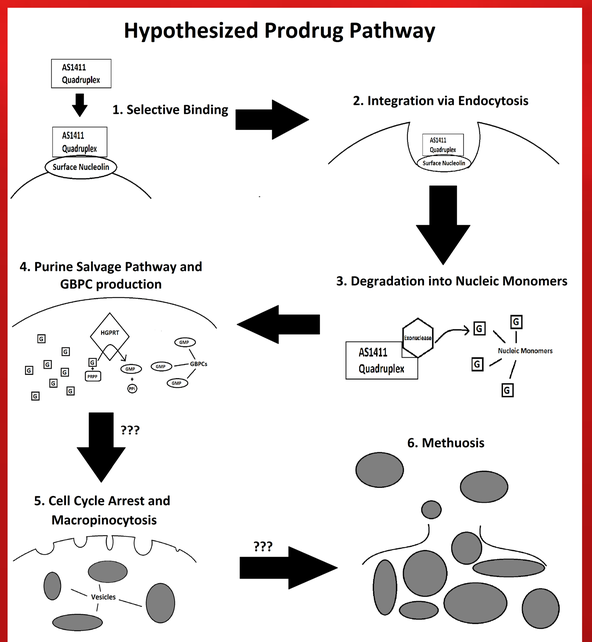

Methods

Cell Culture & HGPRT siRNA Knockdown

A549 cells were cultured in DMEM containing 10% FBS and 1% Penicillin/Streptomycin.

Cells were grown to ~70% confluency and plated onto 96 well plates with 1000 cells per well. Cells were allowed to adhere for 24 hours and transferred to antibiotic free media. Transfection was performed with Lipofectamine 2000 (Fisher Scientific) as described in reagent protocol. Cells were then either untransfected, transfected with HGPRT siRNA (s6887 & s6888, Life Technologies), or transfected with Negative Control #1 siRNA. After 4 hours media was replaced with complete media. Cells were then incubated for 24 or 48 hours as indicated by figure legends.

After transfection, cells were treated with either AS1411, CRO (cytosine-rich negative control oligonucleotide), or sterile water (vehicle control) in concentrations of either 5 or 10 μM as indicated in the figure legends. AS1411 and CRO in the desalted form were purchased from Integrated DNA Technologies (Coralville, IA). Cells treated for 48 hours before being subjected to a MTT colorimetric assay to evaluate levels of proliferation.

BCA Protein Analysis and Western Blot Development Protocol

Cell lysates were prepared on ice with RIPA buffer containing protease and phosphatase inhibitors (Calbiotech, Spring Valley, CA) for 5 min at 4 °C and clarified by centrifugation for 10 min at 14,000 rpm at 4 °C. Protein concentrations were determined using the Pierce™ BCA Protein assay (Fisher Scientific, Waltham, MA) with bovine serum albumin (BSA) standards (Fisher Scientific). Samples for electrophoresis were prepared with 25 μg of protein, 4x loading buffer with 10% β-mercaptoethanol, and distilled water.

Samples were resolved by SDS–PAGE and transferred onto polyvinylidine fluoride (PVDF) membranes (Fisher Scientific) in Tris–glycine transfer buffer (Life Technologies, Grand Island, NY) containing 20% methanol. Membranes were either blocked with 5% milk in tris-buffered saline containing 0.05% tween-20 (TBS-T). The following dilutions were used for primary antibodies: HGPRT 1:500 and α-Tubulin 1:1000. Membranes probed for HGPRT were detected using SuperSignal® West Dura ECL (Fisher Scientific) while α-Tubulin was detected using Pierce® ECL Western Blotting Substrate (Fisher Scientific). Chemiluminescence was visualized using Amersham Hyperfilm™ (GE Healthcare, Little Chalfont, UK) and exposure times are noted in the figure legends.

MTT Colorimetric Assay and Data Analysis

After 48 hours oligonucleotide treatment, MTT (Sigma, St. Louis, MO) was added in the dark at 1/10th total sample volume. Cells were then incubated for 4 hours. Lysis buffer (10% SDS in 0.01 N HCl) was added at half of the original sample volume and incubated overnight to ensure complete lysis and dissolving of crystals. Plates were read at 570 nm and relative absorbance values were exported to Microsoft Excel® for further analysis.

For each MTT assay a 3D bar graph was constructed to compare all test groups relative to one another, as well as an individual bar graph for each transfection type. Each combination of transfection type and treatment group was performed in triplicate. Error bars indicate standard deviation.

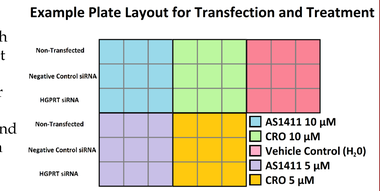

Results & Summary of Findings

Figure 1. Demonstration of HGPRT siRNA Knockdown at 48 Hours

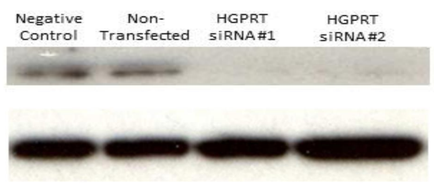

Figure 2. Results of Initial HGPRT siRNA MTT Colorimetric Assay

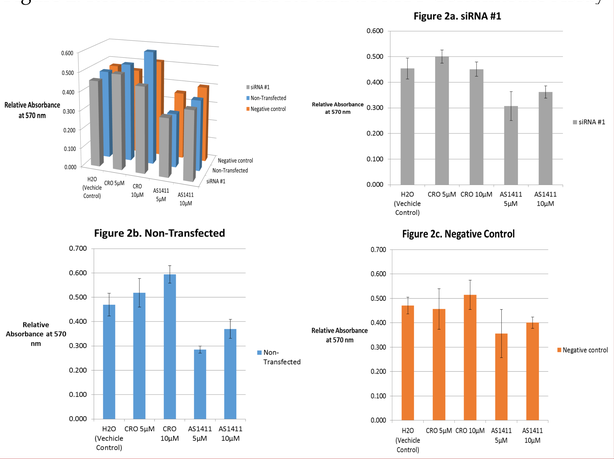

Figure 3. Results of MTT Colorimetric Assay with Doubled Concentration of siRNAs

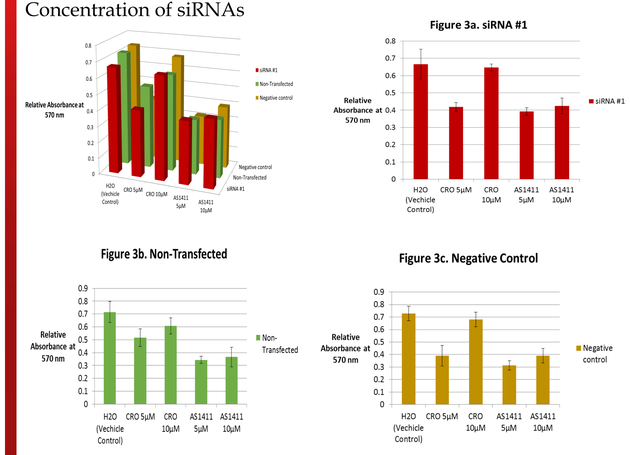

Figure 4. Exploration of HGPRT siRNA Knockdown Longevity

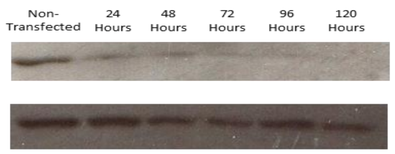

Figure 5. Results of MTT colorimetric assay with transfection time reduced from 48 to 24 hours

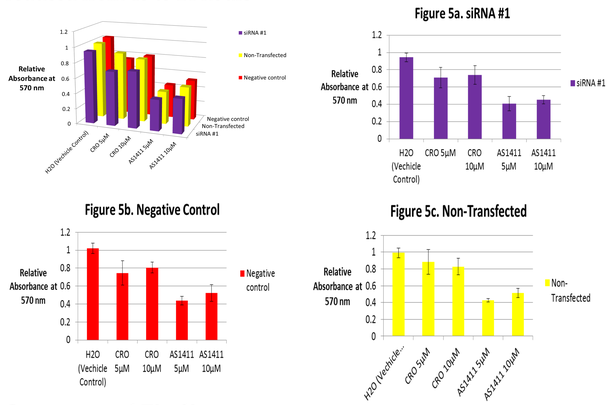

Summary of Findings:

- We successfully used two different siRNAs to knockdown the expression of HGPRT relative to negative control siRNAs.
- HGPRT silencing did not exhibit strong toxic effects on control groups as shown in proliferation assays.
- Concentrations of HGPRT siRNAs utilized were sufficient to induce silencing from 24 hours to 120 hours post-transfection.
- Despite repeated protocol augmentation, HGPRT silencing did not exhibit any significant effects on AS1411's anti-proliferative activity.
- **The data suggests that AS1411 effects are not dependent on HGPRT activity.**

Future Directions & Acknowledgements

Future Directions:

Although these experiments suggest that AS1411 is not dependent upon HGPRT activity in this cell line under a variety of conditions, more experiments are necessary to:

- Confirm that knockdown of HGPRT reduces the antiproliferative activity of GBPCs in this cell line.
- Test in different cell lines, including those that are more sensitive to AS1411 (A549 cells are only moderately sensitive).

Acknowledgements:

- I would like to thank the Bates lab for their instruction, support, and guidance throughout my undergraduate education.
- Additionally, I would like to thank both Dr. Hein and Dr. La Creis Renee Kidd for their work in organizing and running the R25 program here at the University of Louisville.
- This research was funded in part by the National Cancer Institute through the R25 grant program (R25-CA134283).

References

1. Bates, Paula J., Damian A. Laber, Donald M. Miller, Shelia D. Thomas, and John O. Trent. "Discovery and Development of the G-rich Oligonucleotide AS1411 as a Novel Treatment for Cancer." Experimental and Molecular Pathology 86.3 (2009): 151-64. Web.
2. Rosenberg, Jonathan E., Richard M. Bambury, Eliezer M. Van Allen, Harry A. Drabkin, Primo N. Lara, Andrea L. Harzstark, Nikhil Wagle, Robert A. Figlin, Gregory W. Smith, Levi A. Garraway, Toni Choueiri, Fredrik Erlandsson, and Damian A. Laber. "A Phase II Trial of AS1411 (a Novel Nucleolin-targeted DNA Aptamer) in Metastatic Renal Cell Carcinoma." Invest New Drugs Investigational New Drugs 32.1 (2013): 178-87. Web.
3. Zhang, Nan, Tao Bing, Xiangjun Liu, Cui Qi, Luyao Shen, Linlin Wang, and Dihua Shangguan. "Cytotoxicity of Guanine-based Degradation Products Contributes to the Antiproliferative Activity of Guanine-rich Oligonucleotides." Chem. Sci. 6.7 (2015): 3831-838. Web.
4. Garozzo, Roberta, Maria Angela Sortino, Carlo Vancheri, and Daniele Filippo Condorelli. "Antiproliferative Effects Induced by Guanine-based Purines Require Hypoxanthine-guanine Phosphoribosyltransferase Activity." Biological Chemistry 391.9 (2010): n. pag. Web.

Transport and Distribution of Stealth and Cell Penetrating Nanoparticles in Cervical Cancer Tissue Mimics

Maya K. Huss[1*], Lee M. Sims[1*], Julie T. Nguyen[2], Jill M. Steinbach-Rankins[1]
University of Louisville, Department of Bioengineering[1], J. Graham Brown School[2], Equal Contributors*

UNIVERSITY OF LOUISVILLE
J.B. SPEED SCHOOL OF ENGINEERING

Introduction

Background: Cervical cancer is highly prevalent in developing countries, due to insufficient access to health care. Inadequate screening combined with a lack of vaccines often leads to undetected tumors and elevated mortality rates. Relative to preventative options, cervical cancer treatments are often invasive and painful procedures that include surgery, chemotherapy, and radiation. For systemic chemotherapy in particular, it is challenging to achieve distribution within the tumor, thereby harming normal noncancerous cells in the process. As an alternative, polymeric nanoparticles (NPs) may be used as drug and gene delivery vehicles to target and/or enhance the distribution of therapeutic agents in cervical cancer tumors. However, currently there is a lack of *in vitro* methods available to measure and predict therapeutic distribution. To date, *in vivo* studies are the primary method of evaluating distribution; but require limited patient samples and expensive animal models. To circumvent this challenge, three-dimensional (3D) cell culture models can be utilized to create a more physiologically relevant *in vitro* system to assess and predict NP distribution. **Objective:** In this study, our goal was to evaluate the penetration and distribution of stealth and cell penetrating NPs through three types of 3D tumor models: liquid overlay spheroids, hanging drop spheroids, and multicellular layers (MCLs). We used these 3D models of three different cervical cancer cell lines (HeLa, CaSki, and SiHa) to represent different stages of cancer progression: nascent tumors, mid-stage avascular tumors, and stratified epithelial layered tumors. **Hypothesis:** Based on previous studies performed with HeLa cells, we hypothesized that NP co-treatment would offer the greatest penetration and distribution within the tumors, relative to unmodified NPs. **Methods:** To test our hypothesis, we utilized confocal microscopy to image the 3D tumors, and analyzed the images with ImageJ software to evaluate NP distribution within the different tumor types and cell lines. **Results:** We found that MPG and MPG-PEG co-treatment NPs often offered the greatest distribution within the 3D tumor models relative to unmodified NPs. However, NP distribution in the tumors varied based on cell and tumor types, due to their differing sizes and morphologies. **Conclusions:** NP co-treatments offer a promising method to enhance delivery to, and the treatment of cervical cancer. However, tumor composition and morphology must be considered in the early stages of therapeutic screening and development to establish the best treatment type.

Methods

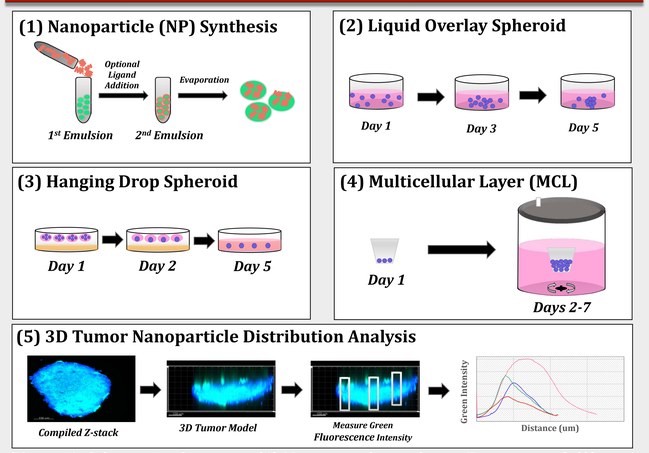

Figure 1. Schematics depicting: (1) Nanoparticle synthesis; Formation of: (2) liquid overlay spheroids, (3) hanging drop spheroids, and (4) multicellular layers; and (5) Nanoparticle distribution using NIH ImageJ software.

Tumor Growth Verification

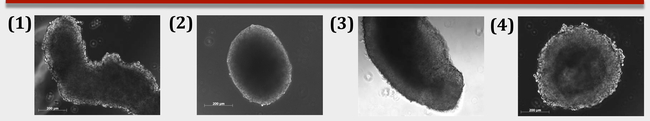

Figure 2. Tumor growth verification imaged using epifluorescence microscopy. Phase contrast images of: (1) HeLa liquid overlay spheroid, (2) CaSki liquid overlay spheroid, (3) SiHa Liquid overlay spheroid, and (4) HeLa hanging drop spheroid.

Results: Spheroid Cross-Sections and Composite Images

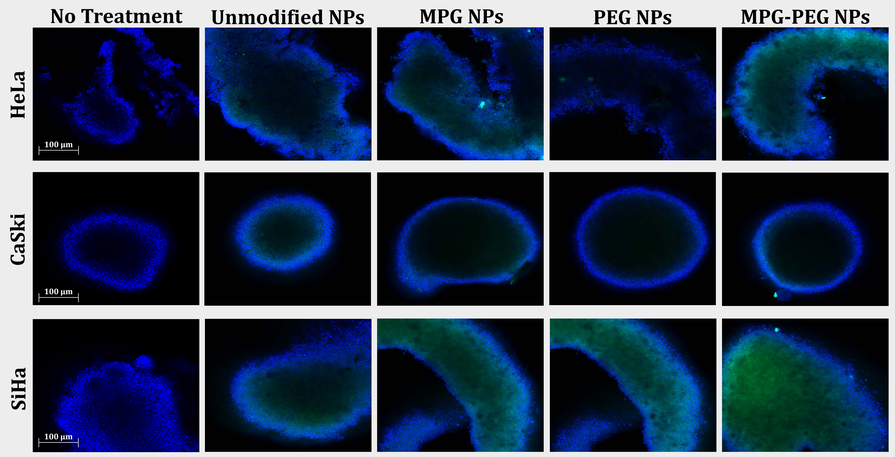

Figure 3. Cross-Sections of Liquid overlay spheroids treated with NPs. Imaged using confocal microscopy.

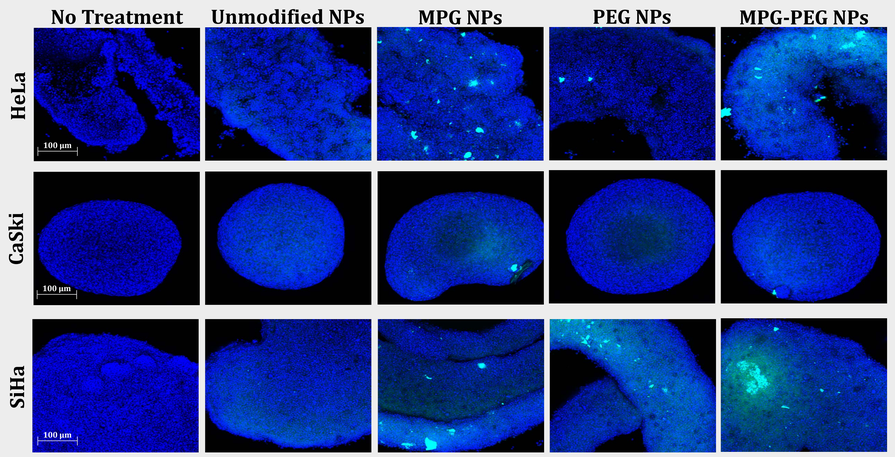

Figure 4. Composite images of Liquid overlay spheroids treated with NPs. Imaged using confocal microscopy.

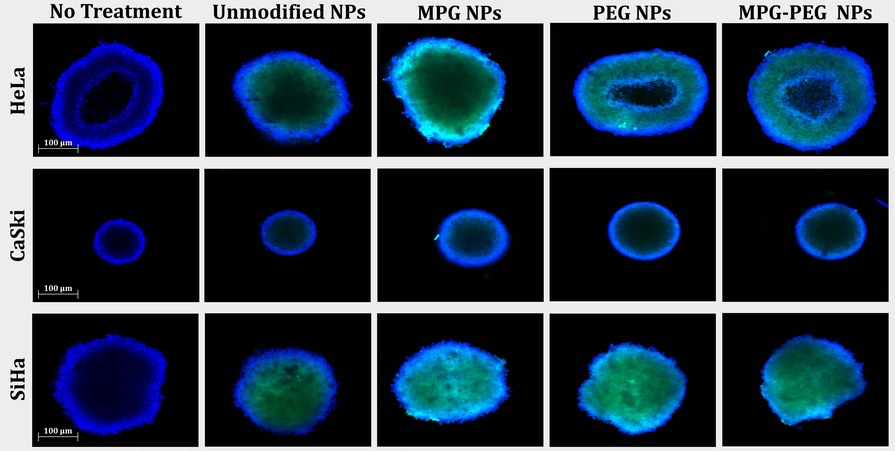

Figure 5. Cross-Sections of Hanging drop spheroids treated with NPs. Imaged using confocal microscopy.

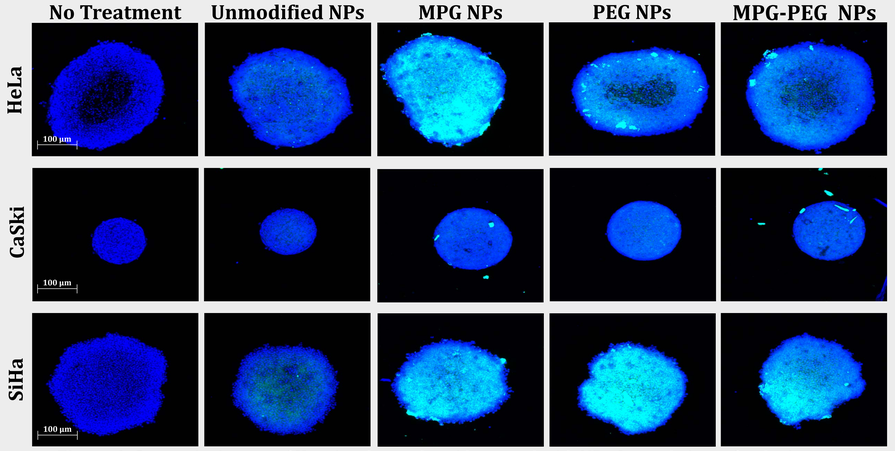

Figure 6. Composite images of Hanging drop spheroids treated with NPs. Imaged via confocal microscopy.

Results: MCL Composite Images

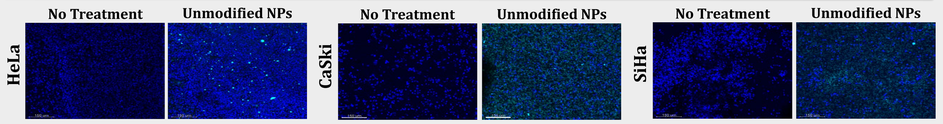

Figure 7. Composite images of Multicellular layers. Imaged via confocal microscopy.
*Note: CaSki and SiHa cells did not form viable multicellular layers.

Results: Quantified Distribution and Penetration of NPs

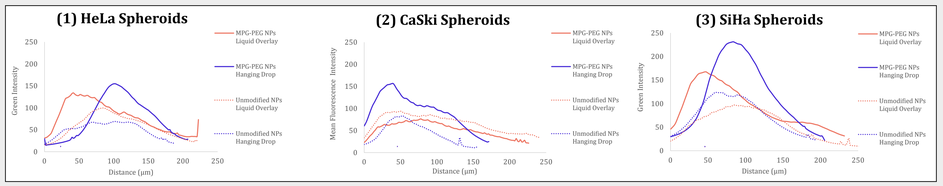

Figure 8. Quantified distribution and penetration of MPG-PEG & Unmodified NPs in: (1) HeLa, (2) CaSki, and (3) SiHa liquid overlay and hanging drop spheroids.

Conclusions & Future Directions

- Between different cell types, NPs in CaSki tumors typically penetrated and distributed less than those in HeLa and SiHa tumors.
- CaSki tumors were smaller and more compact, making NP penetration difficult; whereas, SiHa and HeLa tumors formed more leaky interstitial space, allowing greater distribution of the NPs.
- Hanging drop spheroids had a greater amount of NP distribution and penetration, most likely due to the small size of the tumor models.
- Overall, MPG & PEG NP co-treatment (1/2 dose of each individually administered) demonstrated enhanced distribution and penetration in the 3D tumor models relative to unmodified NPs. *Note: In the CaSki liquid overlay spheroids, unmodified NPs had greater distribution than then MPG & PEG NP co-treatment.
- Since we observed a variation in NP penetration and distribution based on cell line/3D tumor type, tumor composition and morphology are important to consider when evaluating treatment options.
- We are currently testing efficacy with chemotherapeutic nanoparticles in spheroids.
- We are in the process of revising our MCL growth protocol. However, HeLa cells are the primary candidate to move forward in MCL experiments. Once complete, we will test MCL tumor models with MPG NPs, PEG NPs, and MPG & PEG NPs.
- We are currently assessing NP distribution in HeLa MCLs.
- In the future, we plan to evaluate NP distribution and efficacy in *in vivo* cervical cancer models.

Acknowledgements

Research is supported by the University of Louisville Cancer Education Program NIH/NCI R25-CA134283.

Identification of Abrrent Wnt/β-catenin Signaling on Cancer Stem Cell Activation in Hepatocellular Carcinoma

Kevin Jacob[1], Harshul Pandit[1,2], Suping Li[1], Yan Li[1], PhD, Robert C.G. Martin II[1,2], M.D., PhD

[1]Division of Surgical Oncology, Hiram C. Polk Jr. M.D. Department of Surgery, University of Louisville School of Medicine, Louisville, KY
[2] Department of Pharmacology & Toxicology, University of Louisville School of Medicine, Louisville, KY

Introduction

Hepatocellular carcinoma (HCC) is the most common type of liver cancer that, when diagnosed at advanced stage, has a 5-year survival rate of less than 12%. Alarmingly, the recurrence rate of HCC after curative and palliative treatment is 70% in the first 14 months. The most common causes of HCC include HBV, HCV, diabetes, fatty liver disease, and alcoholism. In fact, 18% of patients presenting with cirrhosis in the United States progress to HCC each year. Only 20% of patients qualify for curative treatment (tumor resection) as it is the only treatment option for very early/early stage HCC that is typically asymptomatic. Treatment options for intermediate and advanced stage HCC include chemotherapy with Doxorubicin and Sorafenib. **Cancer Stem Cells (CSCs)** are a subpopulation in the tumor mass. Accumulating evidence suggests that the CSC subpopulation can initiate cancer and drives tumor recurrence, drug resistance, and metastasis. How CSCs are activated is a fundamental question that is not yet completely understood. The **Wnt/β-catenin** pathway is a cardinal pathway contributing to stem-cell organogenesis during embryo development. Multiple studies have identified dysregulation of the Wnt/β-catenin signaling components in epithelial tumors such as HCC. Understanding CSC activation demands attention from the cancer community to identify therapeutic targets for clinical patients and improve patient outcome.

Aim

Aim:

- Identifying canonical Wnt/β-catenin pathway components and/or downstream targets that contribute to activation of CSCs.

Working Hypothesis

Hypothesis: We hypothesize that "β-catenin protein regulates CSCs activation in HCC via the canonical Wnt/β-catenin pathway". We will test this hypothesis with the following experiments:

1. Stabilizing β-catenin in the canonical Wnt pathway will increase oncogenic Wnt downstream products and subsequently will *increase* cancer stem cell properties in HCC cells.
2. Inhibiting Wnt/β-catenin signaling will decrease oncogenic Wnt downstream products and subsequently will *decrease* cancer stem cell properties in HCC cells.

MG132 treatment: MG132 inhibits proteasome degradation → stabilizes β-catenin.
LiCl treatment: LiCl phosphorylates Serine-9 position of GSK3β and inactivates it → stabilizes β-catenin.

XAV939 treatment: XAV939 stabilizes Axin1 and destruction complex → inhibits β-catenin.

LiCl & XAV939 treatment in Control and Serum-Free Hepa1-6 cells

- Inducing spheroid formation (CSC property) by spheroid medium→ Increases β-catenin accumulation and its downstream targets expression.
- LiCl treatment stabilizes β-catenin expression → Increases β-catenin expression and downstream targets compared to control and XAV939 treatments in both the control and spheroid culture cells
- XAV939 stabilizes the destruction complex in the HCC cells → Decreases β-catenin and downstream targets expression compared to control and LiCl treatments in both the control and spheroid culture cells

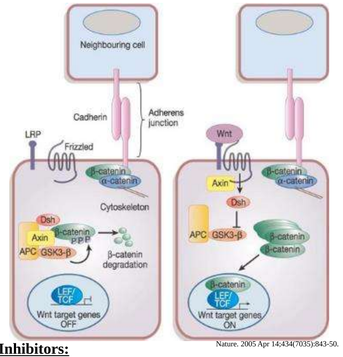

Nature. 2005 Apr 14;434(7035):843-50.

Inhibitors:

- **MG132** → Inhibits proteasome→ *Stabilizes β-catenin*
- **LiCl** → Inhibits GSK3β → *Stabilizes β-catenin*
- **XAV939** → Stabilize Axin1 → *Inhibits β-catenin*

Wnt/β-catenin components: T-GSK3β, p-GSK3β
Downstream Targets of Wnt/β-catenin Pathway:

- **ABCG2:** Drug resistant transporter
- **Cyclin D1:**Oncogene contributing deregulated apoptosis.
- **c-Myc:** Oncogene contributing deregulated apoptosis

Results

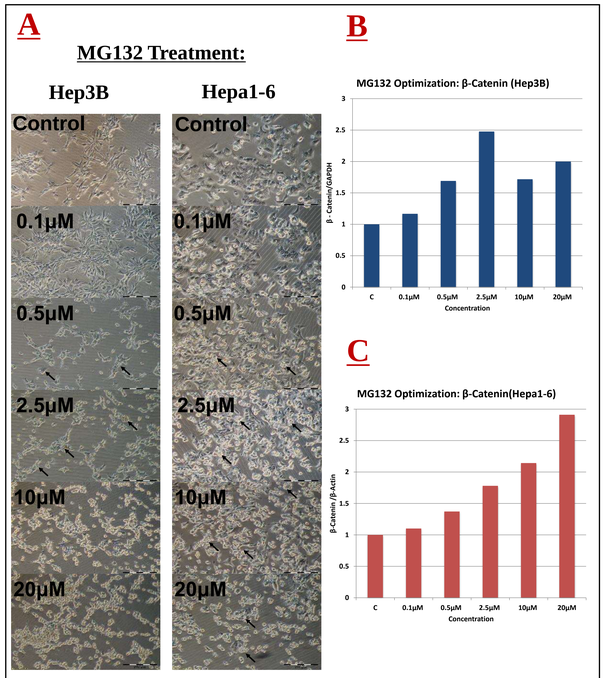

Figure-1: Optimization of MG132 dose. MG132 inhibits proteosomal degradation and stabilizes β-catenin. **(A)** MG132 induces spheroid formation in a dose dependent manner. Images taken at 10X magnification. Black arrows indicate spheroids. Bar = 200 μm. **(B)** Hep3B cells showed a dose dependent increase in β-catenin levels up to 2.5 μM. **(C)** Hepa1-6 cells showed dose dependent increase in β-catenin levels.

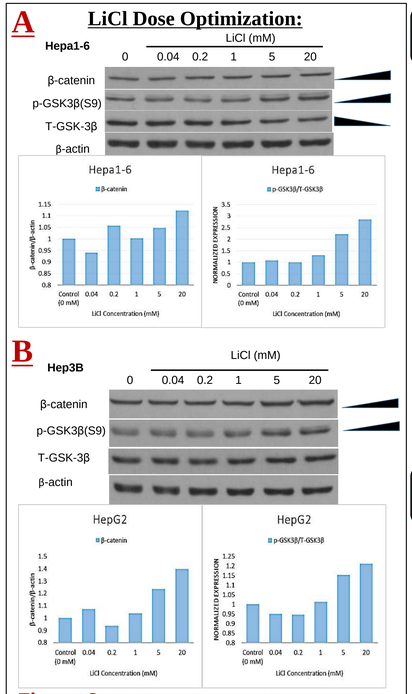

Figure-2: Optimization of LiCl dose. LiCl inhibits GSK3β and stabilizes β-catenin. Western blot analysis showed, **(A)** dose dependent increase in β-catenin expression in Hepa1-6 cell line, and **(B)** dose dependent increase in β-catenin expression in Hep3B cell line. 5 mM is the lowest dose effective in both cell lines.

LiCl (5 mM) and XAV939 (2 μM) Treatment: Control and Spheroid culture (Hepa1-6)

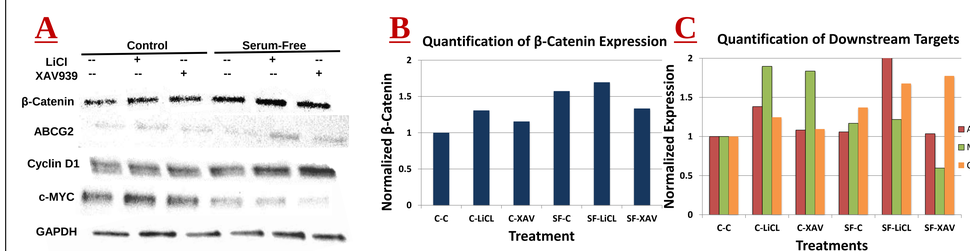

Figure - 3: Canonical Wnt inhibitors affect β-catenin levels in spheroid forming CSC cells. (A) Western blot data showed increase in β-catenin and its downstream targets expression for 5 mM LiCl treated cells in both control and spheroid culture cells. Spheroid culture cells showed increased β-catenin and downstream targets expression relative to control cells. 2 uM XAV939 treated caused decreased β-catenin in spheroid culture but not in control. **(B)** β-catenin expression was semi-quantified and averaged across three replicates and then normalized to both control and GAPDH expression. **(C)** Downstream targets ABCG2, c-MYC, and Cyclin D1 were semi-quantified and normalized.

Methods

Cell Culture:
Hep3B and HepG2 : MEM media + 10% FBS + Antibiotics/Antimycotics.
Hepa1-6: DMEM with 4.5% glucose + 10% FBS + Antibiotics/Antimycotics.
Spheroid culture media (SF) : 1:1 (v/v) DMEM:F12 media without phenol red, 2 mM L-glutamine, 20 ng/mL EGF, 10 ng/mL bFGF, 0.5 % B-27 supplement.

MG132 Dose Optimization (western blot)
Cell Lines: Hep3B and Hepa1-6
Cell Culture Treatment: 18 hour treatment, Control, 0.1μM, 0.5μM, 2.5μM, 10μM, 20μM

LiCl Dose Optimization (western blot)
Cell Lines: Hepa1-6 and HepG2
Cell Culture Treatment: 24 hour treatment, Control, 0.04mM, 0.2mM, 1 mM, 5 mM, 20 mM LiCl

LiCl (5 mM) and XAV939 (2 μM) Treatment (western blot)
Cell Lines: Hepa1-6
Cell Culture: Serum-Free Media, 18 hour treatment
Treatment: Control, C-LiCl, C-XAV, SF-C, SF-LiCl, SF-XAV

Conclusions

- Inhibiting proteasome degradation in the Canonical Wnt/β-catenin pathway induces an increase in β-catenin expression and spheroid formation characteristic of cancer stem cells in Hep3B and Hepa1-6.
- Inhibiting GSK3β, a key component of the Canonical Wnt/β-catenin pathway, induces an increase in both β-catenin expression as well as an increase in downstream targets of the Wnt/β-catenin pathway that are oncogenic properties of cancer stem cells in the Hepa1-6 cell line.
- The unexpected results with respect to the XAV939 treatment in control cells can be attributed to either 1) a lack of optimized treatment dose and time or 2) alternate pathways associated with β-

Future directions

- XAV939 dose optimization experiments.
- siRNA or shRNA mediated knockdown of β-catenin and study effect of canonical Wnt inhibitors.
- TOP/FLASH and FOP/FLASH reporter assays to confirm the findings.

Acknowledgments

Research was supported by the NIH: National Cancer Institute Grant R25-CA-134283.
Special thanks to Dr. Martin's lab for their generous guidance and mentorship and to Dr. Hein and Dr. Kidd for organizing the R25 program at the University of Louisville.

References

1. **El-Serag HB. Hepatocellular carcinoma. N Engl J Med. 2011;365:1118-1127. doi: 10.1056/NEJMra1001683.**
2. **U.S. Cancer Statistics Working Group, *United States Cancer Statistics: 1999– 2010 Incidence and Mortality Web-based Report*, in *www.cdc.gov/uscs*. 2013.**
3. **Forner, A., et al., *Current strategy for staging and treatment: the BCLC update and future prospects.* Semin Liver Dis, 2010. 30(1): p. 61-74.**
4. **Lobo, N.A., et al., *The biology of cancer stem cells.* Annu Rev Cell Dev Biol, 2007. 23: p. 675-99.**
5. **Chiba, T., et al., *Cancer stem cells in hepatocellular carcinoma: Recent progress and perspective.* Cancer Lett, 2009. 286(2): p. 145-53.**

Combining natural compound β-glucan with immune checkpoint inhibitor therapy to promote antitumor immunity

Josephine M. Kim, Anne E. Geller, M.S., Chuanlin Ding, Ph.D., Zan Tong, Ph.D., Jun Yan, M.D., Ph.D.
Department of Medicine, James Graham Brown Cancer Center, University of Louisville

Abstract

Although immune checkpoint inhibitors are a promising approach for facilitating antitumor responses, anti-PD-1 is clinically effective in a limited fraction of advanced lung cancer patients. Therefore, we examined whether β-glucan treatment could act as a potential supplementary therapy to anti-PD-1 immunotherapy, expanding the applicable patient population. The goal of our investigation was to determine whether whole glucan particle (WGP) treatment coupled with PD-1 treatment will result in an enhanced antitumor response compared to either treatment alone. Our in vitro data showed that there was greater proliferation of CD8+ T-cells in the Combination Group than in single treatment or PBS Group. The in vivo data showed that anti-PD-1 and WGP Groups resulted in reduced tumor burden. Both IFN-γ producing CD4+ and CD8+ T-cells were elevated in the single treatment groups in the tumor draining lymph node tissue. However, the Combination Group did not result in synergistic antitumor effect within the treatment period. Further studies are underway to examine whether survival benefits will be provided by WGP and anti-PD-1 combination therapy.

Introduction

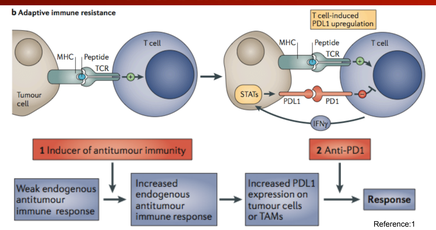

- Tumor cells escape immunosurveillance by expressing the ligands for the PD-1 receptor, PDL1 and PDL2.[1,2]
- PD-1 inhibition decreases down-regulation of effector T cells by tumor cells.[1]
- Clinical trial results indicate that the anti-PD-1 monoclonal antibody is only effective in approximately 20% of advanced non-small-cell lung cancer patients. Therefore, there is a great need for supplementary treatment in order to expand the reach of the anti-PD-1 therapy.[7]

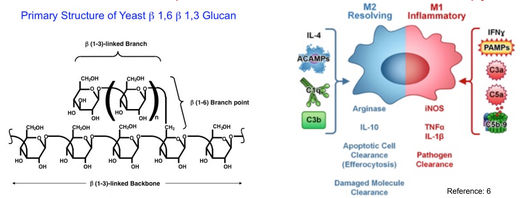

- β-glucan isolated from *Saccharomyces cerevisiae* has displayed antitumor properties such as:
  - The polarization of tumor associated macrophages (TAMs) from the M2 phenotype to the M1 phenotype.[3]
  - Inhibition of myeloid-derived suppressor cell (MDSC) proliferation.[4]
  - Increased tumor cell susceptibility to effector T cell attack. Orally administered whole glucan particles (WGP), which are 85% β-glucan, resulted in over 70% CD8+ T-cell killing activity in tumor-bearing mice, compared to 30% activity in the control.[5]

Methods

In vitro: M2 BMM and OT-1 spleen cell functional assay

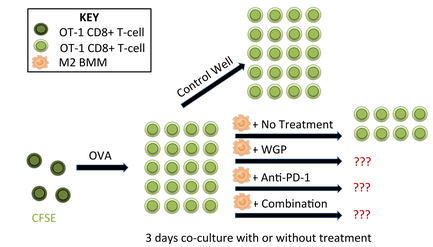

In vivo: 3-week treatment of tumor-bearing mice

Treatment	n
PBS (untreated)	8
WGP β-glucan (800 µg/mouse, oral gavage)	9
Anti-PD-1 mAb (100 µg/mouse, IP injection)	9
WGP β-glucan + anti-PD-1 mAb	10

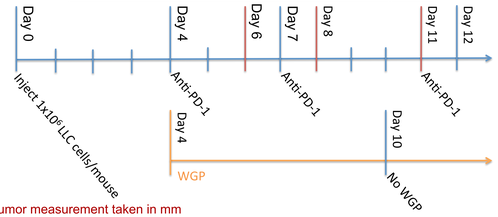

*Tumor measurement taken in mm

Results

Figure 1. OT-1 T-cell proliferation in co-culture with M2 BMM.

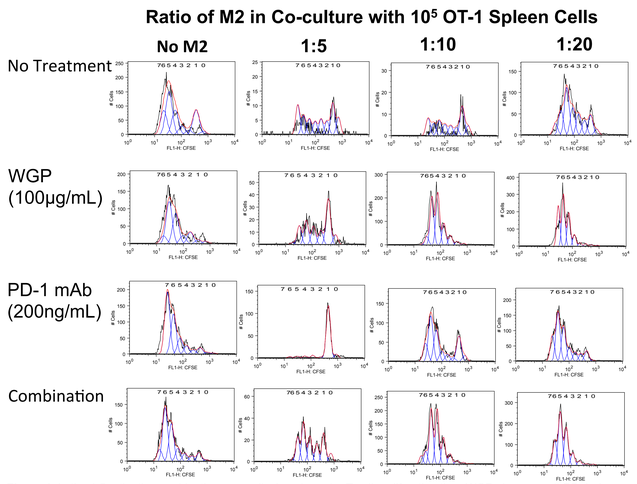

Figure 1. In the 1:5 ratio, the combination group displayed greater T-cell proliferation than WGP alone or anti-PD-1 alone. Spleen cells from OT-1 mice were CFSE-labeled and then co-cultured with M2 BMM in the presence of OVA with or without Anti-PD-1, WGP, or combination treatments.

Figure 2. Tumor diameters of mice treated with PBS, WGP, anti-PD-1, or combination regiments.

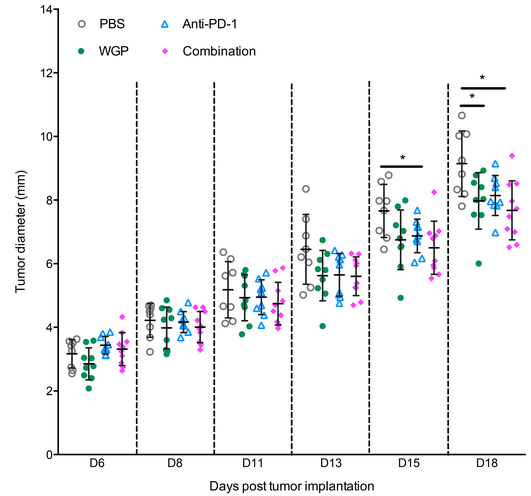

Figure 2. By Day 18, tumor diameter was significantly larger in the PBS Group than in the single treatment groups. Lewis lung carcinoma (LLC) tumor-bearing mice were treated with PBS, WGP, anti-PD-1, or a combination of WGP and anti-PD-1 mAb for three weeks. Anti-PD-1 was intraperitonially injected twice per week, while WGP was administered by oral gavage daily. Tumor diameter was measured three times per week.
*p < 0.05

Figure 3a. Frequency of T_{reg} and IFN-γ producing CD4+ and CD8+ T-cells.

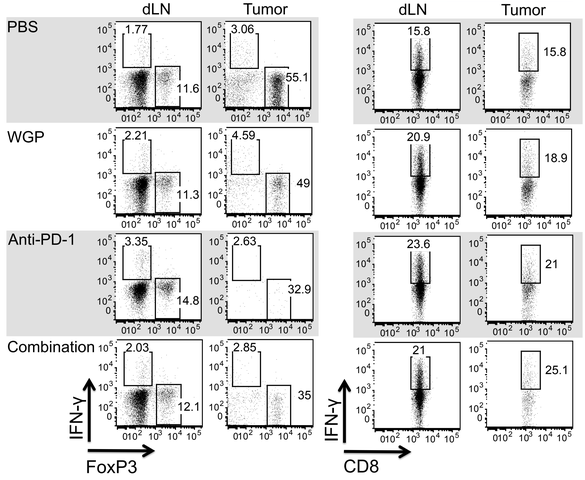

Figure 3b. Summary of frequency of T_{reg} and IFN-γ producing CD4+ and CD8+ T-cells.

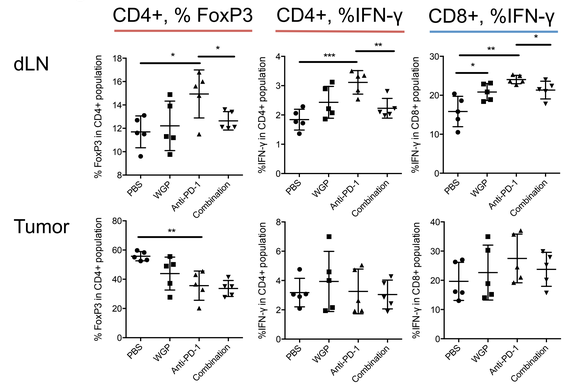

Figure 3. In the draining lymph node tissue (dLN), the percent of IFN-γ producing CD8+ T-cells was significantly higher in the single treatment groups than in the PBS group. In the dLN, the combination group exhibited a similar percentage of immune suppressive and stimulatory activity as in the WGP Group.

Conclusions

- In vitro co-culture studies showed that WGP and anti-PD-1 combination therapy resulted in elevated CD8+ T-cell proliferation compared to the single treatment groups at the 1:5 M2 versus OT-1 T-cell ratio.
- In vivo studies indicated that both WGP alone and anti-PD-1 alone treatments result in reduced tumor burden. However, Combination therapy did not display a synergistic effect in tumor reduction.
- In vivo treatment with WGP alone and anti-PD-1 alone treatments resulted in elevated percentages of IFN-γ producing CD4+ and CD8+ T-cells in tumor draining lymph nodes.

Future Directions

- Current studies are underway to determine the survivor benefit of combination therapy.
- The results of this investigation were in concurrence with a previous study indicating that anti-PD-1 treatment is not very effective on LLC tumors. Future experiments will examine the effectiveness of WGP and anti-PD-1 combination therapy on other tumor models.[8]
- Larger sample groups of mice may help to deter the statistical effect of the large variations in tumor diameter observed across groups.

References

1. Pardoll, D. M. The blockade of immune checkpoints in cancer immunotherapy. *Na t Rev. Cancer* 12 (2012):252–64.
2. Dunn, G. P., A. T. Bruce, H. Ikeda, L. J. Old, and R. D. Schreiber. 2002. Cancer immunoediting: from immunosurveillance to tumor escape. Nat. Immunol. 3: 991–998.
3. Liu, Min, et al. "Dectin-1 Activation by a Natural Product β-Glucan Converts Immunosuppressive Macrophages into an M1-like Phenotype." *The Journal of Immunology* 195.10 (2015): 5055-5065.
4. Albeituni, S. H., C. Ding, M. Liu, X. Hu, F. Luo, G. Kloecker, M. Bousamra, H.-G. Zhang, and J. Yan. "Yeast-Derived Particulate β-Glucan Treatment Subverts the Suppression of Myeloid-Derived Suppressor Cells (MDSC) by Inducing Polymorphonuclear MDSC Apoptosis and Monocytic MDSC Differentiation to APC in Cancer." *The Journal of Immunology* 196.5 (2016): 2167-180.
5. Li, B., Cai, YH., Qi, CJ., Hansen, R., Ding, CL., Mitchell, TC., and Yan J.: 2010. Orally Administrated Particular β-Glucan Modulates Tumor-capturing Dendritic Cells and Improves Anti-tumor T Cell Responses in Cancer. *Clinical Cancer Research*, 16(21):5153-64. PMCID: 2970627
6. Bohlson, S. S., S. D. O'Conner, H. J. Hulsebus, M.-M. Ho, and D.A. Fraser. "Complement, C1q, and C1q-Related Molecules Regulate Macrophage Polarization." *Frontiers in Immunology* 5 (2014): n. pag.
7. Garon, E. B., et al. "Pembrolizumab for the Treatment of Non–Small-Cell Lung Cancer." *The New England Journal of Medicine* 372 (2015): 2018-28.
8. Barnes, S., de Marval, P. M., Hauser, J., Brainard, T., Small, D., Synnott, A., and R. Mullin. "A Systematic Evaluation of Immune Checkpoint Inhibitors." AACR 2015. Charles River Discovery Services. Morrisville, NC, USA. Poster Presentation.

Acknowledgements

This research was supported by the R25-CA134283 grant from the National Cancer Institute through the University of Louisville Cancer Education Program.

The Impact of Complex Interactions of Chemokine Sequence Variants on Prostate Cancer Risk among men of African Descent.

Tiana L. Martin[1], Christian P. Bradley, Dominique Jones-Reed , LaCreis R. Kidd,
Department of Pharmacology & Toxicology and James Graham Brown Cancer Center

INTRODUCTION

Role of Chemokines in Inflammatory/Immune Response and Cancer

- Chemokines belong to a family of small chemoattractant cytokines that mediate their effects by binging to protein-coupled receptors.
- Chemokine-chemokine receptor pairs trigger leukocyte production, which promotes cell survival and metastasis.
- Certain chemokine-cytokine receptor pairs are elevated in cancer
- Chemokines have several roles:
  - Lure cancer cells and chemokine receptor bearing immune cells (T and dendritic cells) to an inflamed site to promote lymph node metastasis
  - Mediate acute and chronic inflammation
  - Promote chemotaxis (cell movement), tumor growth and metastasis
  - Facilitate dendritic cell functions
  - Regulate angiogenesis
- Genetic alterations detected in coding and regulatory regions of chemokine associated genes may alter macromolecules (mRNA/protein express, chemokine-chemokine receptor production/function, protein-protein interactions), cellular behavior and ultimately modify PCa risk.

RESEARCH GAP

The impact of two or more genetic alterations detected in chemokine and chemokine receptor genes on prostate cancer (PCa) susceptibility remains understudied.

RESEARCH OBJECTIVES

Evaluate the individual and joint modifying effects of chemokine associated sequence variants in relation to PCa risk among men of African Descent.

HYPOTHESIS

Men who inherit two or more sequence variants (linked with a pro-inflammatory response, cell survival, cell proliferation, immune/tumor cell migration, chemotaxis, invasion, angiogenesis, and lymph node metastasis) will have increased PCa risk relative to those with the wildtype genotype.

MATERIALS AND METHODS

Study Design

- Using a case-control study design, we evaluated the independent and joint modifying effects of 43 sequence variants detected in chemokine associated genes in relation to PCA risk.
- 814 Men of African Descent (279 cases, 535 controls) were recruited from cancer screening programs, hospitals, or cancer centers located in the Washington D.C., South Carolina, and Kingston, Jamaica.
- Chemokine SNPs were detected and evaluated in germ-line DNA using Illumina's Veracode genotyping system.
- Genetic data was generated by Expression Analysis, Inc. (http://expressionanalysis.com/)

Statistical Design

- Compared the frequency distribution of genotypes between cases and controls using the chi-square test.
- Risk estimates associated with inheritance of at least one minor chemokine-associated sequence variant allele were expressed as odds ratios (ORs) and corresponding 95% Confidence Intervals (95%CI) using unconditional multivariate LR models, adjusted for age.
- MDR was used to evaluate individual and joint modifying effects innate immunity SNPs in relation to PCa risk (http://epistasis.org/). Combined effects were restricted to the total and U.S. population.
- Individual and gene combination effects were performed using SAS 9.4 and multi-factor dimensionality reduction (http://epistasis.org/), respectively.
- Adjustments for multiple hypothesis testing were made using false discovery rate (FDR) and permutation testing.

BIOLOGICAL RATIONALE

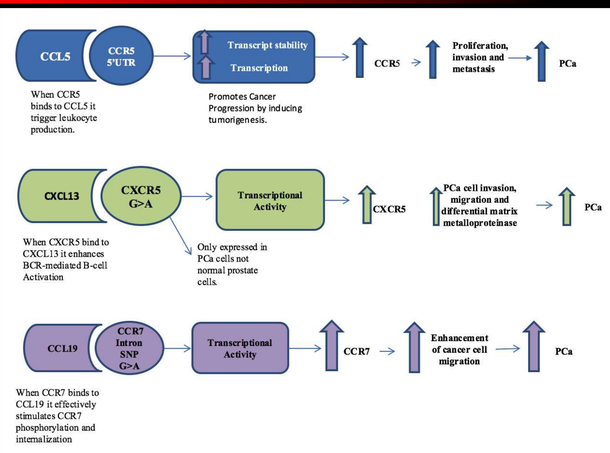

CLINICAL IMPACT

- By studying complex gene-gene interactions of these various chemokine sequence variants we hope to identify new biomarkers that can be used for effective treatments of aggressive forms of PCa and development of targeted drugs to the specific sites.
- This study could also lead to a more accurate detection of PCa and help develop early screening strategies for this disease.

RESULTS

Table 2. Association between selected Chemokine-Related Sequence Variants and PCa Risk among Men of African Descent.

Gene dbSNP ID Location predicted function	Genotype	Cases n (%)	Controls n (%)	Adjusted OR (95% CI)	p-value	P-trend
CCL5	GG	111 (13.65)	150 (18.45)	1.00 (referent)		0.001
rs2107538	GA	124 (15.25)	270 (33.21)	0.72 (0.49, 1.06)	0.005	
5' near gene	AA	44 (5.41)	114 (14.02)	0.53 (0.32, 0.89)	0.003	
TFBS	(AA+GA)	168 (20.66)	384 (47.23)	0.66 (0.46, 0.96)	0.001	
	AA vs (GG+GA)			0.64 (0.41, 1.02)	0.057	
CCR7	AA	55 (6.77)	151 (18.57)	1.00 (referent)		0.031
rs3136685	GA	139 (17.10)	237 (29.15)	1.87 (1.19, 2.94)	0.011	
Intron 1	GG	85 (10.46)	146 (17.96)	1.40 (0.84, 2.29)	0.022	
	(GG+GA)	224 (27.55)	383 (47.11)	1.66 (1.08, 2.54)	0.348	
	GG vs (AA+GA)			0.92 (0.62, 1.35)	0.008	
CCL5	TT	114 (14.02)	147 (18.08)	1.00 (referent)		0.002
rs3817655	TA	115 (14.15)	278 (34.19)	0.56 (0.38, 0.83)	0.0001	
Intron 2	AA	49 (6.03)	110 (13.53)	0.52 (0.32, 0.87)	0.007	
TFBS	TT vs (AA+TA)	164 (20.17)	388 (47.72)	0.56 (0.38, 0.81)	0.317	
	AA vs (TT+TA)			0.74 (0.47, 1.16)	0.0001	
CCR5	AA	85 (10.55)	194 (24.07)	1.00 (referent)		0.004
rs1799988	GA	107 (13.28)	227 (28.16)	0.84 (0.56, 1.26)	0.644	
UTR'5	GG	85 (10.55)	108 (13.40)	1.39 (0.88, 2.18)	0.002	
TFBS	(GG+GA)	192 (23.82)	335 (41.56)	1.01 (0.70, 1.46)	0.0901	
	GG vs (AA+GA)			1.52 (1.02, 2.26)	0.0013	
CCL2	AA	169 (20.79)	345 (42.44)	1.00 (referent)		0.525
rs1024611	GA	103 (12.67)	168 (20.66)	1.52 (1.04, 2.18)	0.146	
TFBS	GG	7 (0.86)	21 (2.58)	1.16 (0.39, 3.44)	0.392	
	(GG+GA)	110 (13.53)	189 (23.25)	1.46 (1.02, 2.12)	0.257	
	GG vs (AA+GA)			1.00 (0.34, 2.92)	0.294	
CXCR2	GG	230 (28.29)	434 (53.38)	1.00 (referent)		0.793
rs11574752	GA	43 (5.29)	99 (12.18)	0.88 (0.55, 1.42)	0.61	
miRNA(miRanda)	AA	6 (5.74)	1 (0.12)	38.11 (3.81, 380.89)	0.002	
	(AA+GA)	49 (6.03)	100 (12.30)	1.066 (0.67, 1.67)	0.002	
	AA vs (GG+GA)			38.88 (3.89, 388.23)	0.782	
CCR7	AA	84 (10.32)	173 (21.25)	1.00 (referent)		0.458
rs3136687	GA	153 (18.80)	249 (30.59)	1.44 (0.97, 2.14)	0.161	
Intron 1	GG	42 (5.16)	113 (13.88)	0.96 (0.572, 1.62)	0.234	
	(GG+GA)	195 (23.96)	362 (44.47)	1.29 (0.88, 1.89)	0.037	
	GG vs (AA+GA)			0.76 (0.48, 1.20)	0.516	

†Denotation of Abbreviations: Exonic splicing enhancer (ESE) or exonic splicing silencer (ESS) binding sites; MicroRNAs (miRNA), Transcription factor binding site (TFBS, UTR (Untranslated Region).

Table 3. Association between Selected Chemokine-Related Sequence Variants and PCa Risk among U.S. Men of African Descent.

Genes dbSNP ID Location Predicted Function	Genotype	Cases n (%)	Controls n (%)	Adjusted OR (95% CI)	p-value	p-trend
CXCR7	AA	62 (10.32)	204 (33.94)	1.00 (referent)		0.038
rs1045879	GA	87 (14.48)	185 (30.78)	1.27 (0.81, 2.00)	0.028	
Exon 1	GG	20 (3.33)	43 (7.15)	0.99 (0.46, 2.16)	0.176	
cds-synon	(GG+GA)	107 (17.80)	228 (37.94)	1.25 (0.80, 1.93)	0.499	
	GG vs (AA+GA)			0.89 (0.42, 1.84)	0.019	
CCL25	AA	108 (17.91)	232 (38.47)	1.00 (referent)		0.034
rs2032887	GA	52 (8.62)	166 (27.53)	0.701 (0.44, 1.11)	0.044	
Exon 3	GG	10 (1.66)	35 (5.80)	0.570 (0.22, 1.42)	0.195	
Splicing (ESE or ESS)	(GG+GA)	62 (10.28)	201 (33.33)	0.679 (0.44, 1.05)	0.357	
	GG vs (AA+GA)			0.650 (0.26, 1.60)	0.002	
nsSNP probably damaging missense R>H					0.027	
CCL5	GG	73 (12.11)	123 (20.40)	1.00 (referent)		0.002
rs2107538	GA	71 (11.77)	220 (36.48)	0.67 (0.42, 1.08)	0.007	
5' near gene	AA	26 (4.31)	90 (14.93)	0.53 (0.28, 1.01)	0.125	
TFBS	(AA+GA)	97 (16.09)	310 (51.41)	0.63 (0.40, 0.99)	0.013	
	AA vs (GG+GA)			0.67 (0.37, 1.20)	0.001	
CCL5	AA	121 (20.13)	261 (43.43)	1.00 (referent)		0.018
rs2280789	GA	42 (6.99)	150 (24.96)	0.59 (0.36, 0.96)	0.304	
Intron 1	GG	6 (1.00)	21 (3.49)	0.99 (0.34, 2.98)	0.488	
TFBS	(GG+GA)	48 (7.99)	171 (28.45)	0.64 (0.40, 1.01)	0.028	
	GG vs (AA+GA)			1.18 (0.39, 3.48)	0.010	
CCL5	TT	77 (12.77)	121 (20.07)	1.00 (referent)		0.003
rs3817655	TA	63 (10.45)	227 (37.65)	0.49 (0.30, 0.80)	0.176	
Intron 2	AA	30 (4.98)	85 (14.10)	0.54 (0.29, 1.02)	0.0001	
TFBS	TT vs (AA+TA)	93 (15.42)	312 (51.74)	0.51 (0.32, 0.80)	0.577	
	AA vs (TT+TA)			0.81 (0.46, 1.42)	0.022	
CXCR5	GG	59 (9.78)	185 (30.68)	1.00 (referent)	0.0001	0.058
rs523604	GA	83 (13.76)	193 (32.01)	1.67 (1.04, 2.69)		
Intron 1	AA	28 (4.64)	55 (9.12)	1.86 (0.960, 3.60)	0.133	
	(AA+GA)	111 (18.41)	248 (41.13)	1.72 (1.09, 2.69)	0.228	
	AA vs (GG+GA)			1.40 (0.76, 2.56)	0.090	
CCR6	GG	119 (19.83)	318 (53.00)	1.00 (referent)	0.072	0.199
rs3093023	GA	43 (7.17)	101 (16.83)	1.20 (0.72, 1.99)		
Intron 1	AA	8 (1.33)	11 (1.83)	3.25 (1.02, 10.32)	0.512	
	(AA+GA)	51 (8.50)	112 (18.67)	1.34 (0.83, 2.16)	0.157	
	AA vs (GG+GA)			3.07 (0.98, 9.66)	0.182	
CCR7	AA	36 (5.97)	132 (21.89)	1.00 (referent)	0.327	0.293
rs3136687	GA	100 (16.58)	203 (33.67)	1.73 (1.02, 2.92)		
Intron 1	GG	34 (5.64)	98 (16.25)	1.18 (0.62, 2.20)	0.008	
	(GG+GA)	134 (22.22)	301 (49.92)	1.54 (0.94, 2.52)	0.482	
	GG vs (AA+GA)			0.82 (0.48, 1.37)	0.379	
CCR5	AA	57 (9.56)	158 (26.51)	1.00 (referent)	0.022	0.076
rs1799988	GA	62 (10.40)	181 (30.37)	0.71 (0.43, 1.17)		
UTR'5	GG	50 (8.39)	88 (14.77)	1.10 (0.63, 1.92)	0.880	
TFBS	(GG+GA)	112 (18.79)	269 (45.13)	0.81 (0.52, 1.26)	0.019	
	GG vs (AA+GA)			1.29 (0.78, 2.12)	0.042	
CCL1	TT	37 (6.15)	127 (21.10)	1.00 (referent)		0.108
rs2282691	TA	92 (15.28)	212 (35.22)	1.79 (1.04, 3.08)	0.070	
Intron Variant	AA	41 (6.81)	93 (15.45)	1.58 (0.84, 2.96)	0.112	
	TT vs (AA+TA)	133 (22.09)	305 (50.66)	1.72 (1.03, 2.87)	0.593	
	AA vs (TT+TA)			1.07 (0.64, 1.75)	0.492	

Table 4. Association between selected Chemokine-Related Sequence Variants and PCa Risk among Jamaican Men

Genes dbSNP ID Location Predicted function	Genotype	Cases n (%)	Controls n (%)	Adjusted OR (95% CI)	p-value	p-trend
CCR5	GG	28 (13.33)	36 (17.14)	1.00 (referent)		0.041
rs1799987	GA	46 (21.90)	46 (21.90)	1.19 (0.58, 2.42)	0.506	
Intron 1	AA	34 (16.19)	20 (9.52)	2.07 (0.93, 4.64)	0.047	
TFBS	(AA+GA)	80 (38.10)	66 (31.43)	1.55 (0.81, 2.98)	0.142	
	AA vs (GG+GA)			1.92 (0.96, 3.88)	0.050	
CCR5	AA	28 (13.33)	36 (17.14)	1.00 (referent)		0.036
rs1799988	GA	45 (21.43)	46 (21.90)	1.17 (0.57, 2.38)	0.551	
TFBS	GG	35 (16.67)	20 (9.52)	2.11 (0.94, 4.71)	0.038	
	(GG+GA)	80 (38.10)	66 (31.43)	1.55 (0.81, 2.98)	0.142	
	GG vs (AA+GA)			1.96 (1.04, 3.70)	0.036	
CCL17	GG	48 (22.75)	52 (24.64)	1.00 (referent)		0.132
rs223895	GA	46 (21.80)	43 (20.38)	1.23 (0.64, 2.34)	0.613	
	AA	15 (7.11)	7 (3.32)	3.65 (1.20, 11.01)	0.092	
	(AA+GA)	61 (28.91)	50 (23.70)	1.505 (0.82, 2.76)	0.313	
	AA vs (GG+GA)			3.28 (1.14, 9.42)	0.107	
CCR7	AA	11 (5.21)	21 (9.95)	1.00 (referent)		0.086
rs3136685	GA	53 (25.12)	45 (21.33)	2.78 (1.09, 7.08)	0.056	
	GG	45 (21.33)	36 (17.06)	2.52 (0.97, 6.52)	0.045	
	(GG+GA)	98 (46.45)	81 (38.39)	2.66 (1.10, 6.41)	0.372	
	GG vs (AA+GA)			1.16 (0.62, 2.15)	0.037	

Table 5. Evaluation of Main Effects and Interactions of Chemokine SNPs as Predictors of Pca among U.S. Men of African Descent using MDR.

Best Model (dbSNPID#)	Interactions	Cross Validation Consistency (CVC)	Average Testing Accuracy (ATA)	Permutation Testing p-value
One Factor				
CCL5_rs3817655	51	6	0.577	0.0875
Two Factor				
CCL24_rs2302004 CCL5_rs3817655	1275	6	0.6182	0.0125
Three Factor				
CCR5_rs2227010 CCR7_rs3136687 CXCR5_rs523604	20,825	10	0.6889	<0.001

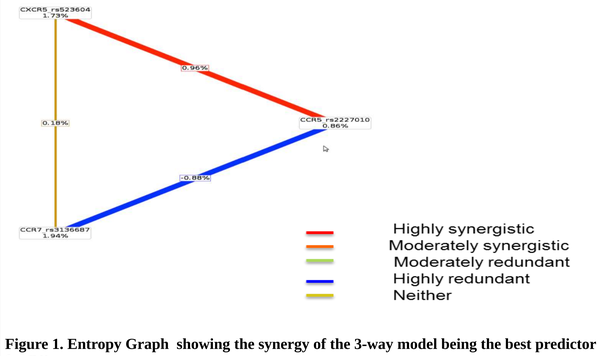

Figure 1. Entropy Graph showing the synergy of the 3-way model being the best predictor for PCa .

SUMMARY

- A complex interaction along the CCR5-CXR5-CCR7 axis was identified as the best 3-factor Pca predictor, following MDR Analysis.
- Upon closer inspection of entropy graphs, this 3-factor model did not reveal synergistic effects in relation to PCa. However, we cannot rule out the possibility of additive effects.
- None of the pairwise combinations (CXCR5-CCR5, CXCR5-CCR7, CCR5-CCR7) provided any more information than each SNP when considered alone based on analysis of individual and combined information gain scores.
- Assessment of the CCR5 rs227010, CXR5 rs3136687 and CCR7 rs523604 were not individually related to Pca.

FUTURE DIRECTIONS

- Identify and validate novel chemokine-associated SNPs as effective predictors of prostate cancer risk, disease progression, disease/biochemical recurrence, and overall survival within a larger and ethnic diverse sub-population.
- *In vitro* and *in vivo* studies are needed to understand the mechanism by which chemokine associated genes (e.g., CCL5, CCR5 and CCR7) alter prostate cancer outcomes

ACKNOWLEDGEMENTS

- We thank Rick Kittles, Maria Jackson and others for contributing study participants from Washington D.C., South Carolina and Jamaica.
- Grant/Research support: National Cancer Institute grant R25-CA-134283, Clinical Translational Science Pilot Grant to LRK, "Our Highest Potential" in Cancer Research Endowment to LRK, and P20-MD000175 NIH MCMHD to KSK.